ELSEVIER

www.elsevier.nl/locate/jorganchem

Journal of Organometallic Chemistry 587 (1999) 176–180

Journal of Organometallic Chemistry

Reactivity of $[Et_4N]_2[MeSb\{Fe(CO)_4\}_3]$ toward HOAc and $[Cu(MeCN)_4]BF_4$: formation of $[Et_4N][Me(OAc)Sb\{Fe(CO)_4\}_2]$ and $[MeSb\{Fe(CO)_4\}\{Fe_2(CO)_8\}]$

Minghuey Shieh [a,*], Li-Fang Ho [a], Jiann-Jang Cherng [a], Chuen-Her Ueng [a],
Shie-Ming Peng [b], Gene-Hsiang Lee [c]

[a] *Department of Chemistry, National Taiwan Normal University, Taipei 116, Taiwan, ROC*
[b] *Department of Chemistry, National Taiwan University, Taipei 107, Taiwan, ROC*
[c] *Instrumentation Center, National Taiwan University, Taipei 107, Taiwan, ROC*

Received 16 March 1999; received in revised form 18 May 1999

Abstract

Reactions of the tetrahedral methylantimony complex $[Et_4N]_2[MeSb\{Fe(CO)_4\}_3]$ with HOAc and $[Cu(MeCN)_4][BF_4]$ were investigated. While the reaction of $[Et_4N]_2[MeSb\{Fe(CO)_4\}_3]$ with HOAc forms the substituted complex $[Et_4N][Me(OAc)Sb\{Fe(CO)_4\}_2]$ ($[Et_4N]$[**I**]), the treatment with $[Cu(MeCN)_4][BF_4]$ forms the oxidized product $[MeSb\{Fe(CO)_4\}\{Fe_2(CO)_8\}]$ (**II**). The structures of $[Et_4N]$[**I**] and **II** are determined by single-crystal X-ray diffraction. $[Et_4N]$[**I**] crystallizes in the orthorhombic space group $Pna2_1$ with $a = 16.627(4)$, $b = 9.411(3)$, $c = 17.347(4)$ Å, $V = 2714(1)$ Å^3, and $Z = 4$. The crystals of **II** are triclinic, space group $P\bar{1}$ with $a = 9.335(1)$, $b = 10.313(3)$, $c = 10.372(1)$ Å, $\alpha = 97.46(1)$, $\beta = 93.63(1)$, $\gamma = 94.65(1)°$, $V = 984.0$ (3) Å^3, and $Z = 2$. Cluster **I** is an OAc group substituted product which displays a tetrahedral metal core with the central antimony atom bonded to two $Fe(CO)_4$ fragments, one Me group, and one OAc moiety. Compound **II** is the two-electron oxidized product of $[Et_4N]_2[MeSb\{Fe(CO)_4\}_3]$ where one Fe–Fe bond is formed upon the addition of $[Cu(MeCN)_4][BF_4]$. The results are compared with those of the analogous bismuth system and the role of the main group elements is discussed as well.

Keywords: Antimony; Carbonyl; Iron; X-ray diffraction

---

1. Introduction

Main group-transition metal carbonyl clusters attract extensive attention due to their interesting bonding modes and reactivity patterns [1]. To understand the reactivity of metal clusters, their reactions towards acids [1] and oxidants such as $[Cu(MeCN)_4]BF_4$ [1,2] have been well documented. Recent study has shown that the role of the main group elements has significant influence on the reactivity of the mixed main group-transition metal clusters [3]. We have been interested in the interaction of main group-transition metal clusters with organic moieties and have investigated the alkylations of the tetrahedral clusters $[Et_4N]_3[E\{Fe(CO)_4\}_4]$ (E = Bi, Sb) with a series of alkyl halides [4]. The monoalkylated products $[Et_4N]_2[RE\{Fe(CO)_4\}_3]$ (E = Bi, Sb) were obtained from these reactions. In the bismuth system, treatments of $[Et_4N]_2[RBi\{Fe(CO)_4\}_3]$ with HCl (aq.) yielded the decomposed products; however, the reaction with the mild acid HOAc led to the cyclic complexes $[RBiFe(CO)_4]_2$. On the other hand, the reactions of $[Et_4N]_2[RBi\{Fe(CO)_4\}_3]$ with $[Cu(MeCN)_4][BF_4]$ underwent severe bond breakage to give the decomposition products as well [4b]. To probe the effect of HOAc and $[Cu(MeCN)_4][BF_4]$ and the role of the main group element in these reactions, we further investigated the reactions of the analogous monoalkylated antimony cluster $[Et_4N]_2[MeSb\{Fe(CO)_4\}_3]$ with HOAc and $[Cu(MeCN)_4][BF_4]$, which are compared with the outcome of the Bi–Fe system.

---

* Corresponding author. Fax: + 886-2-29324249.

0022-328X/99/$ - see front matter
PII: S0022-328X(99)00291-0

2. Experimental

2.1. General methods

All reactions were performed under an atmosphere of pure nitrogen using standard Schlenk techniques [5]. Solvents were purified, dried, and distilled under nitrogen prior to use. The compound $[Et_4N]_2[MeSb\{Fe(CO)_4\}_3]$ was prepared according to the published method [4c]. IR spectra were recorded on a Perkin–Elmer Paragon 500 spectrometer as solutions in CaF_2 cells. The ^1H- and ^{13}C-NMR spectra were taken on a Jeol 400 (400 MHz) instrument. Elemental analyses were performed on a Perkin–Elmer 2400 analyzer at the NSC Regional Instrumental Center at National Taiwan University, Taipei, Taiwan.

2.2. Reaction of $[Et_4N]_2[MeSb\{Fe(CO)_4\}_4]$ with HOAc

To a sample of 0.792 g (0.879 mmol) of $[Et_4N]_2[MeSb\{Fe(CO)_4\}_3]$ was added 5.0 ml of HOAc. The mixed solution was stirred and heated in an oil bath at 50°C for 65 h. The solution was filtered and HOAc was then removed under vacuum, and the residue was then washed with hexanes and extracted with ether. The ether extract was recrystallized with ether/hexanes to give 0.21 g (0.317 mmol) of a yellowish orange product $[Et_4N][Me(OAc)Sb\{Fe(CO)_4\}_2]$ ($[Et_4N]$[**I**]) (36%). IR (νCO, MeCN): 2040 m, 2017 s, 1930 vs, br cm^{-1}. ^1H-NMR (400 MHz, DMSO-d_6, 298 K): δ 1.61 (s, 3H), 1.73 (s, 3H) (chemical shifts not given for $[Et_4N]^+$). Anal. Calc. for $[Et_4N][Me(OAc)Sb\{Fe(CO)_4\}_2]$: C, 34.48; H, 3.96; N, 2.12. Found: C, 34.35; H, 3.75; N, 2.05%.

Table 1
Crystallographic data for $[Et_4N][Me(OAc)Sb\{Fe(CO)_4\}_2]$ ($[Et_4N]$[**I**]) and $[MeSb\{Fe(CO)_4\}\{Fe_2(CO)_8\}]$ (**II**)

	$[Et_4N]$[**I**]	**II**
Empirical formula	$C_{19}H_{26}Fe_2NO_{10}Sb$	$C_{13}H_3Fe_3O_{12}Sb$
Formula weight	641.69	640.44
Crystal system	Orthorhombic	Triclinic
Space group	$Pna2_1$	$P\bar{1}$
a (Å)	16.627(4)	9.335(1)
b (Å)	9.411(3)	10.313(3)
c (Å)	17.347(4)	10.372(1)
α (°)		97.46(1)
β (°)		93.63(1)
γ (°)		94.65(1)
V (Å^3)	2714(1)	984.0(3)
Z	4	2
D_{calc} (Mg m^{-3})	1.570	2.162
Absorption coefficient (cm^{-1})	20.826	49.5
Diffractometer	Nonius (CAD4)	Nonius (CAD4)
Radiation (λ) (Mo–K$_\alpha$) (Å)	0.7107	0.7107
Temperature (°C)	25	25
T_{min}/T_{max}	0.78/1.00	0.44/1.00
Residuals, R [a], Rw [a]	0.033, 0.031	0.027, 0.029

[a] The functions minimized during least-squares cycles were $R = \Sigma|F_o - F_c|/\Sigma F_o$ and $Rw = [\Sigma w(F_o - F_c)^2/\Sigma w(F_o)^2]^{1/2}$.

2.3. Reaction of $[Et_4N]_2[MeSb\{Fe(CO)_4\}_4]$ with $[Cu(MeCN)_4][BF_4]$

To a solution of 0.630 g (0.70 mmol) of $[Et_4N]_2[MeSb\{Fe(CO)_4\}_3]$ in 30 ml of THF was added 0.458 g (1.46 mmol) of $[Cu(MeCN)_4][BF_4]$. The mixed solution was stirred at room temperature for 63 h. The solution was filtered, the solvent was removed under vacuum, and the residue was then extracted with hexanes. The hexanes extract was chromatographed using hexanes as eluent to give the greenish brown product which was recrystallized with ether/hexanes to give 0.11 g (0.17 mmol) of yellowish orange complex $[MeSb\{Fe(CO)_4\}\{Fe_2(CO)_8\}]$ (**II**) (25%). IR (νCO, hexanes): 2106 m, 2061 s, 2039 s, 2028 s, 2010 w, sh, 1975 w, 1944 m, br cm^{-1}. ^1H-NMR (400 MHz, $CDCl_3$, 298 K): δ 2.34 (s, 3H). ^{13}C-NMR (100 MHz, $CDCl_3$, 298 K): δ 6.37, 206.3, 213.4. Anal. Calc. for $[MeSb\{Fe(CO)_4\}\{Fe_2(CO)_8\}]$: C, 24.38; H, 0.47. Found: C, 24.52; H, 0.48. M.p. 104°C (dec.).

2.4. X-ray structural characterization of complexes $[Et_4N]$[I] and II

A summary of selected crystallographic data for $[Et_4N]$[**I**] and **II** is given in Table 1. All crystals were mounted on glass fibers with Epoxy cement. Data collection was carried out on a Nonius CAD4 diffractometer using graphite-monochromated Mo–K$_\alpha$ radiation at 25°C. A ψ scan absorption correction was made [6]. Data reduction and structural refinement were performed using the NRCC-SDP-VAX packages [7], and atomic scattering factors were taken from the International Tables for X-ray Crystallography [8].

Structures of $[Et_4N]$[**I**] and **II**. The orange crystal of $[Et_4N]$[**I**] chosen for diffraction measurement was ca. 0.10 × 0.45 × 0.55 mm, and brown crystal **II** had dimensions 0.50 × 0.20 × 0.15 mm. Cell parameters were obtained from 25 reflections with 2θ angle in the range 19.00–26.10° for $[Et_4N]$[**I**], and $23.38° < 2\theta < 32.48°$ for **II**. A total of 1867 reflections with $I > 2.0\sigma(I)$ for $[Et_4N]$[**I**] (3060 reflections with $I > 2.5\sigma(I)$ for **II**) were used in the refinement. The structures were solved by the heavy atom method and refined by least-squares cycles. All the non-hydrogen atoms were refined with anisotropic temperature factors. Full-matrix least-squares refinement led to convergence with $R = 3.3$ and $Rw = 3.1\%$ for $[Et_4N]$[**I**], and with $R = 2.7$ and $Rw = 2.9\%$ for **II**.

Table 2
Selected bond distances (Å) and bond angles (°) for $[Et_4N][Me(OAc)Sb\{Fe(CO)_4\}_2]$ ($[Et_4N][\mathbf{I}]$)

Bond distances			
Sb–Fe(1)	2.509(2)	Sb–Fe(2)	2.505(2)
Sb–C(9)	2.151(8)	Sb–O(9)	2.077(6)
C(10)–O(9)	1.34 (1)	C(10)–O(10)	1.19 (1)
Bond angles			
Fe(1)–Sb–Fe(2)	131.55(5)	Fe(1)–Sb–C(9)	106.2(2)
Fe(1)–Sb–O(9)	107.4(2)	Fe(2)–Sb–C(9)	107.2(2)
Fe(2)–Sb–C(9)	107.2(2)	Fe(2)–Sb–O(9)	108.0(2)

Table 3
Selected bond distances (Å) and bond angles (°) for $[MeSb\{Fe(CO)_4\}\{Fe_2(CO)_8\}]$ (**II**)

Bond distances			
Sb–Fe(1)	2.5543(9)	Sb–Fe(2)	2.549(1)
Sb–Fe(3)	2.5160(9)	Sb–C(13)	2.162 (5)
Fe(1)–Fe(2)	2.847(1)		
Bond angles			
Fe(1)–Sb–Fe(2)	67.83(3)	Fe(1)–Sb–Fe(3)	130.18(3)
Fe(1)–Sb–C(13)	110.0(2)	Fe(2)–Sb–Fe(3)	127.78(3)
Fe(2)–Sb–C(13)	112.0(2)	Fe(3)–Sb–C(13)	105.2(2)

The selected distances and angles of $[Et_4N][\mathbf{I}]$ and **II** are given in Tables 2 and 3, respectively.

3. Results and discussion

3.1. Reaction of $[Et_4N]_2[MeSb\{Fe(CO)_4\}_3]$ with HOAc and $[Cu(MeCN)_4]BF_4$

The previous study showed that the monoalkylated bismuth complexes $[Et_4N]_2[RBi\{Fe(CO)_4\}_3]$ formed the cyclic products $[RBi\{Fe(CO)_4\}]_2$ when treated with HOAc (R = Et, Pr, Bu); and in the Me case, the corresponding cyclic compound was also formed presumably via the methylbismuth complex [4b]. The function of HOAc is of interest because there is no acetate ligand incorporated into these clusters, which are in contrast to those of $Ru_3(CO)_{12}$ with carboxylic acids RCO_2H (R = H, Me, or Et) [9] and other related diruthenium-based metal carbonyls [10]. According to the products from the Bi–Fe–CO system, HOAc acts more like an oxidizing agent to induce the cluster fragmentation and reformation. However, an interesting question arises if HOAc ever ligates to the Bi–Fe clusters in the course of the reaction. To attempt to answer this question, we decided to treat the analogous complex $[Et_4N]_2[MeSb\{Fe(CO)_4\}_3]$ with HOAc due to the similar chemical property of Sb and Bi in some cases [1,4c]. This reaction, however, led to the formation of the OAc-substituted tetrahedral complex $[Et_4N][Me(OAc)Sb\{Fe(CO)_4\}_2]$ ($[Et_4N][\mathbf{I}]$) instead of forming the corresponding antimony cyclic complex $[MeSb\{Fe(CO)_4\}]_2$.

In the bismuth case, the formation of $[RBi\{Fe(CO)_4\}]_2$ is proposed to result from the dimerization of $RBi\{Fe(CO)\}_4$ derived from $[RBi\{Fe(CO)_4\}_3]^{2-}$. This study indicates that, in the antimony case, the OAc^- group behaves more importantly as a nucleophile toward the central antimony atom, presumably in the +5 oxidation state, to replace one $Fe(CO)_4$ group to form cluster **I**. This difference is intriguing and could be attributed to the stronger Sb–O versus Bi–O bond, which results in the formation of the four-coordinated antimony product **I** in the Sb case rather than undergoing further fragmentation and dimerization to give the ring complex as in the Bi system. The result may suggest that the OAc^- might ligate to the bismuth atom in the Bi–Fe system to form the reactive species $[R(OAc)Bi\{Fe(CO)_4\}_2]^-$ followed by acetate removal, Bi–Fe bond breakage, and dimerization to give the cyclic complexes.

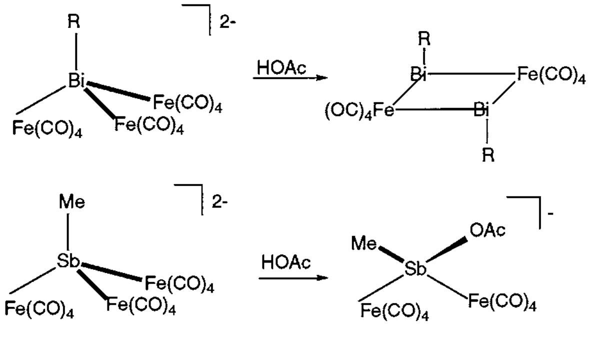

I

It has been shown that most metal clusters can be oxidized by $[Cu(MeCN)_4]BF_4$ to cause metal–metal bond formation or metal–vertex loss to give rise to the oxidized products. However, the extent of oxidation is mainly dependent on the nature of the metal–metal bonds [2]. In the bismuth case, the monoalkylated bismuth compounds $[Et_4N]_2[RBi\{Fe(CO)_4\}_3]$ with $[Cu(MeCN)_4]BF_4$ induced severe bond breakage/formation to give the decomposed complexes [4b]. In this study, if $[Et_4N]_2[MeSb\{Fe(CO)_4\}_3]$ was treated with two equivalents of $[Cu(MeCN)_4]BF_4$, one Fe–Fe bond was formed to give the tetrahedral neutral complex $[MeSb\{Fe(CO)_4\}\{Fe_2(CO)_8\}]$ (**II**). Compound **II** is obviously the two-electron oxidized product of the tetrahedral dianionic compound $[Et_4N]_2[MeSb\{Fe(CO)_4\}_3]$. Again, the differing outcomes could be ascribed to the stronger Sb–R and Sb–Fe bonds compared with those in bismuth system due to the smaller size of Sb versus Bi.

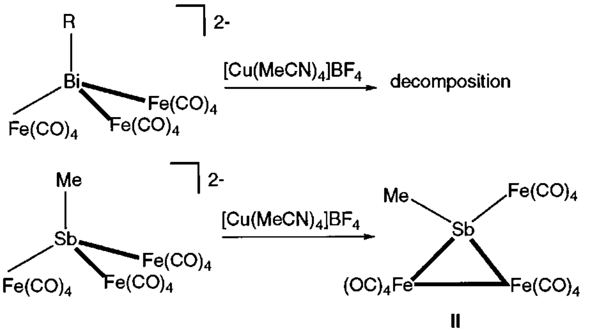

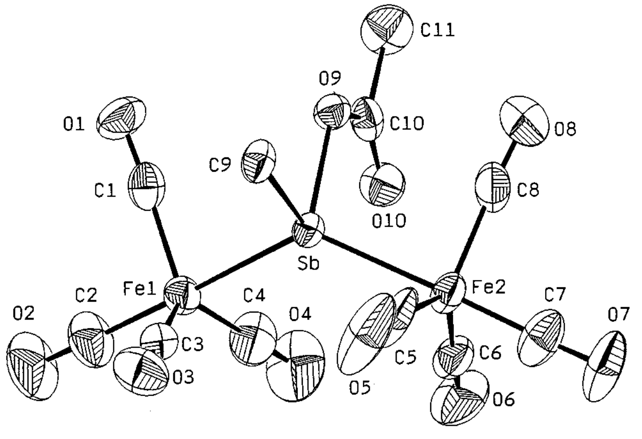

Fig. 1. ORTEP diagram showing the structure and atom labeling for **I**.

3.2. Structures of complexes [Et_4N][**I**] and **II**

As shown in Figs. 1 and 2, the antimony atoms in the clusters **I** and **II** are in the distorted tetrahedral environment. This type of structure is seen in some Sb–Fe carbonyl clusters [4c,11] and clusters **I** and **II** provide the new additions to this family. For comparison, the average Fe–Sb–Fe angle (without Fe–Fe bonds), the Sb–Fe distance, and the Sb–C length of the related tetrahedral clusters are listed in Table 4. As shown in Table 4, the Sb–C lengths are close to the sum of single bond covalent radii (2.2 Å) [12] and compared well with those in the related clusters [4c]. The Sb–Fe distances in **I** and **II** are in the range of other known Sb–$Fe(CO)_4$ distances (2.460–2.715 Å) [11,13,14] and are compared to those found in other structurally characterized antimony complexes such as $[ClSb\{Fe(CO)_2Cp\}_3]_2^{2+}$ (2.539 Å, average) [15] and $[Cl_2Sb\{Fe(CO)_2Cp\}_2]^+$ (2.440 Å, average) [16].

The Fe–Sb–Fe angle (131.55(5)°) in cluster **I** is greater than the corresponding angles in $[Me_2Sb\{Fe(CO)_4\}_2]^-$ (123.95(4)°) and $[MeISb\{Fe(CO)_4\}_2]^-$ (122.20(7)°) [4c,11b]. This is caused by the less steric hindrance of the OAc group than the Me or I fragment because in cluster **I** the OAc group is almost perpendicular to the Fe–Sb–Fe plane. For the monosubstituted Sb–Fe clusters, the average Fe(1)–Sb–Fe(2) angle (128.98°) in **II** is significantly greater than that in $[MeSb\{Fe(CO)_4\}_3]^{2-}$ (114.43°). This is attributable to the existence of an $Fe_2(CO)_8$ moiety that contains an Fe–Fe bond. Moreover, cluster **II** is structurally related to the previously reported cluster $[SbFe_4(CO)_{16}]^-$ [14a], in which the tetrahedral Sb atom is bonded to two $Fe(CO)_4$ fragments and the $Fe_2(CO)_8$ moiety. The acute Fe–Sb–Fe angle (with Fe–Fe bond) in **II** (67.83(3)°) is greater than the corresponding angle of

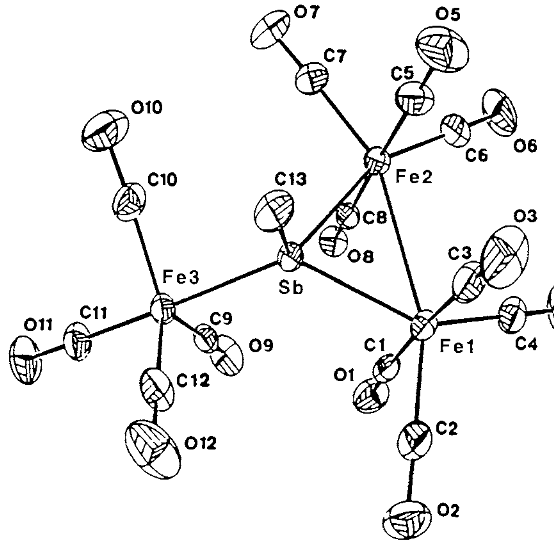

Fig. 2. ORTEP diagram showing the structure and atom labeling for **II**.

Table 4
Comparison of the average Fe–Sb–Fe angle (without Fe–Fe bonds) and the average Sb–Fe and Sb–C distances in the related clusters

Compounds	Fe–Sb–Fe angle (°)	Sb–Fe (Å)	Sb–C (Å)	Ref.
$[Et_4N]_3[Sb\{Fe(CO)_4\}_4]$	109.56	2.666	–	[11a]
$[Et_4N]_2[MeSb\{Fe(CO)_4\}_3]$	114.43	2.614	2.160(7)	[4c]
$[Et_4N][Me_2Sb\{Fe(CO)_4\}_2]$	123.95(4)	2.53	2.146	[4c]
$[PPN][MeISb\{Fe(CO)_4\}_2]$	122.20(7)	2.508 (1)	–	[11b]
$[Me_4N][SbFe_4(CO)_{16}]$	113.13	2.603	–	[14a]
[Et_4N][**I**]	131.55(5)	2.507	2.151(8)	This work
II	128.98	2.540	2.162(5)	This work

$[SbFe_4(CO)_{16}]^-$ (62.09(3)°) due to the smaller steric hindrance of the methyl group than the $Fe(CO)_4$ group.

Finally, in cluster **I**, the acetato ligand OAc binds to the Sb atom in the η^1-fashion and this type of bonding mode is less seen than the commonly observed η^2-OAc in the diruthenium complexes such as $[Ru_2(CO)_4(\mu\text{-}O_2CR)(DPPM)_2]^+$, $[Ru_2(CO)_4(\mu\text{-}O_2CR)(DPPE)_2]^+$, $[Ru_2(\mu\text{-}Pz')(\mu\text{-}O_2CMe)(CO)_4(HPz')_2]$, and $[Ru_2(\mu\text{-}Pz')(\mu\text{-}O_2CMe)(CO)_4(PPh_3)_2]$ [10]. It is noted that the C(10)–O(10) distance (1.19(1) Å) is significantly shorter than that (1.34 (1) Å) of C(10)–O(9), the one involving bonding to Sb, due to the chelating effect.

4. Summary

The reaction of $[Et_4N]_2[MeSb\{Fe(CO)_4\}_3]$ with HOAc forms the OAc substituted cluster **I** while treatment with $[Cu(MeCN)_4]BF_4$ produces cluster **II**. These results are somewhat different from those of the corresponding reactions in the Bi–Fe system due to the smaller size and larger basicity of the antimony versus the bismuth atom.

5. Supplementary material

Additional crystallographic data of $[Et_4N]$[**I**] and **II** are available from the authors.

Acknowledgements

We thank the National Science Council of the Republic of China for financial support (NSC87-2113-M-003-001).

References

[1] For recent reviews of transition-metal/main-group compounds, see: (a) W.A. Herrmann, Angew. Chem. Int. Ed. Engl. 25 (1986) 56. (b) M.D. Vaira, P. Stoppioni, M. Peruzzini, Polyhedron 6 (1987) 351. (c) O.J. Scherer, Comments Inorg. Chem. 6 (1987) 1. (d) O.J. Scherer, Angew. Chem. Int. Ed. Engl. 24 (1985) 924. (e) K.H. Whitmire, J. Coord. Chem. 17 (1988) 95. (f) G. Huttner, K. Knoll, Angew. Chem. Int. Ed. Engl. 26 (1987) 743. (g) G. Huttner, K. Evertz, Acc. Chem. Res. 19 (1986) 406. (h) H. Vahrenkamp, Adv. Organomet. Chem. 22 (1983) 169. (i) A.H. Cowley, J. Organomet. Chem. 400 (1990) 71. (j) A.-J. Dimaio, A.L. Rheingold, Chem. Rev. 90 (1990) 169. (k) K.H. Whitmire, J. Clust. Sci. 2 (1991) 231. (l) K.H. Whitmire, Adv. Organomet. Chem. 42 (1997) 1. (m) P. Mathur, Adv. Organomet. Chem. 41 (1997) 243. (n) M. Shieh, J. Clust. Sci. 10 (1999) 3.

[2] (a) C.B. Lagrone, K.H. Whitmire, M.R. Churchill, J.C. Fettinger, Inorg. Chem. 25 (1986) 2080. (b) K.H. Whitmire, M. Shieh, C.B. Lagrone, B.H. Robinson, M.R. Churchill, J.C. Fettinger, R.F. See, Inorg. Chem. 26 (1987) 2798. (c) K.H. Whitmire, C.B. Lagrone, M.R. Churchill, J.C. Fettinger, B.H. Robinson, Inorg. Chem. 26 (1987) 3491.

[3] (a) L.E. Bogan, Jr., T.B. Rauchfuss, A.L. Rheingold, J. Am. Chem. Soc. 107 (1985) 3843. (b) L.E. Bogan, Jr., G.R. Clark, T.B. Rauchfuss, Inorg. Chem. 25 (1986) 4050. (c) M. Shieh, T.-F. Tang, S.-M. Peng, G.-H. Lee, Inorg. Chem. 34 (1995) 2797 and Refs. therein.

[4] (a) M. Shieh, Y. Liou, S.-M. Peng, G.-H Lee, Inorg. Chem. 32 (1993) 2212. (b) M. Shieh, Y. Liou, B.-W. Jeng, Organometallics 12 (1993) 4926. (c) M. Shieh, C-M. Sheu, L.-F. Ho, J.-J. Cherng, L.-F. Jang, C.-H. Ueng, Inorg. Chem. 35 (1996) 5504.

[5] D.F. Shriver, M.A. Drezdon, The Manipulation of Air Sensitive Compounds, Wiley, New York, 1986.

[6] A.C.T. North, D.C. Philips, F.S. Mathews, Acta Crystallogr. Sect. A 24 (1968) 351.

[7] E.J. Gabe, Y. Lepage, J.P. Charland, F.L. Lee, P.S. White, J. Appl. Crystallogr. 22 (1989) 384.

[8] International Tables for X-ray Crystallography, vol. IV, Kynoch Press, Birmingham, UK, 1974.

[9] G.R. Crook, B.F.G. Johnson, J. Lewis, I.G. Williams, G. Gamlen, J. Chem. Soc. A (1969) 2761.

[10] (a) W.G. Klemperer, B. Zhong, Inorg. Chem. 32 (1993) 5821. (b) S.J. Sherlock, M. Cowie, E. Singleton, M.M. de V. Steyn, Organometallics 7 (1988) 1663. (c) K.-B. Shiu, C.-H. Li, T.-J. Chan, S.-M. Peng, M.-C. Cheng, S.-L. Wang, F.-L. Liao, M.Y. Chiang, Organometallics 14 (1995) 524. (d) K.-B. Shiu, W.-M. Lee, C.-L. Wang, S.-L. Wang, F.-L. Liao, J.-C. Wang, L.-S. Liou, S.-M. Peng, G.-H. Lee, M.Y. Chiang, Organometallics 15 (1996) 2979.

[11] (a) S. Luo, K.H. Whitmire, Inorg. Chem. 28 (1989) 1424. (b) J.W. van Hal, J.L. Stark, K.H. Whitmire, J. Organomet. Chem. 557 (1998) 163.

[12] J.E. Huheey, E.A. Keiter, R.L. Keiter, Inorganic Chemistry: Principles of Structure and Reactivity, Harper Collins College Publishers, New York, 1993.

[13] (a) A.H. Cowley, N.C. Norman, M. Pakulski, D.L. Bricker, D.H. Russell, J. Am. Chem. Soc. 107 (1985) 8211. (b) A.M. Arif, AH. Cowley, M. Pakulski, J. Chem. Soc. Chem. Commun. (1987) 622.

[14] (a) S. Luo, K.H. Whitmire, J. Organomet. Chem. 376 (1989) 297. (b) K.H. Whitmire, J.S. Leigh, S. Luo, M. Shieh, M.D. Fabiano, New J. Chem. 12 (1988) 397. (c) A.L. Rheingold, S.J. Gieb, M. Shieh, K.H. Whitmire, Inorg. Chem. 26 (1987) 463.

[15] Trinh-Toan, L.F. Dahl, J. Am. Chem. Soc. 93 (1971) 2654.

[16] F.W.B. Einstein, R.D.G. Jones, Inorg. Chem. 12 (1973) 1690.